Journal of Biomedical Optics

BiomedicalOptics.SPIEDigitalLibrary.org

In vivo characterization of light scattering properties of human skin in the 475- to 850-nm wavelength range in a Swedish cohort

Hanna Jonasson
Ingemar Fredriksson
Sara Bergstrand
Carl Johan Östgren
Marcus Larsson
Tomas Strömberg

Hanna Jonasson, Ingemar Fredriksson, Sara Bergstrand, Carl Johan Östgren, Marcus Larsson, Tomas Strömberg, "*In vivo* characterization of light scattering properties of human skin in the 475- to 850-nm wavelength range in a Swedish cohort," *J. Biomed. Opt.* **23**(12), 121608 (2018), doi: 10.1117/1.JBO.23.12.121608.

Journal of Biomedical Optics 23(12), 121608 (December 2018)

In vivo characterization of light scattering properties of human skin in the 475- to 850-nm wavelength range in a Swedish cohort

Hanna Jonasson,[a,b,*] Ingemar Fredriksson,[a,c] Sara Bergstrand,[b] Carl Johan Östgren,[b] Marcus Larsson,[a] and Tomas Strömberg[a]
[a]Linköping University, Department of Biomedical Engineering, Linköping, Sweden
[b]Linköping University, Department of Medical and Health Sciences, Linköping, Sweden
[c]Perimed AB, Järfälla, Stockholm, Sweden

Abstract. We have determined *in vivo* optical scattering properties of normal human skin in 1734 subjects, mostly with fair skin type, within the Swedish CArdioPulmonary bioImage Study. The measurements were performed with a noninvasive system, integrating spatially resolved diffuse reflectance spectroscopy and laser Doppler flowmetry. Data were analyzed with an inverse Monte Carlo algorithm, accounting for both scattering, geometrical, and absorbing properties of the tissue. The reduced scattering coefficient was found to decrease from 3.16 ± 0.72 to 1.13 ± 0.27 mm^{-1} (mean ± SD) in the 475- to 850-nm wavelength range. There was a negative correlation between the reduced scattering coefficient and age, and a significant difference between men and women in the reduced scattering coefficient as well as in the fraction of small scattering particles. This large study on tissue scattering with mean values and normal variation can serve as a reference when designing diagnostic techniques or when evaluating the effect of therapeutic optical systems. [DOI: 10.1117/1.JBO.23.12.121608]

Keywords: optical properties; tissue; skin; scattering; spectroscopy.

Paper 180394SSR received Jun. 29, 2018; accepted for publication Aug. 31, 2018; published online Sep. 28, 2018.

1 Introduction

Diagnostic optical modalities detect and analyze backscattered photons from illuminated tissue. The common principle for these techniques is that the detected light contains information on tissue scattering and absorption from the interrogated tissue volume. To untangle this information, one needs to understand how the optical properties are related to photon propagation in tissue. Therapeutic modalities on the other hand, depositing light energy in tissue, are also influenced by the means for light delivery and tissue light transport governed by the optical properties.

Photon propagation in tissue is commonly modeled using either the diffusion approximation or Monte Carlo simulations. Although the former can be calculated analytically, the latter is considered most accurate.[1] Both approaches predict remitted light intensity given that the absorbing and scattering properties are known. In skin tissue, melanin and hemoglobin are the most dominant absorbing chromophores in the visible wavelength range. The main sources of tissue scattering are filamentous proteins such as keratins in the epidermis and collagen in the dermis,[2] or intracellular structures such as nuclei and mitochondria.[3] The size of the scattering particles also has a direct impact on the scattering angle, affecting both the scattering phase function for a given wavelength and how the reduced scattering coefficient, μ_s', varies with wavelength.[4] In some cases, the scattering properties themselves have been shown to contain physiological information of high importance, for example, in cancer[5] and when assessing burn wounds.[6] It has also been suggested that the fraction of large and small scattering particles in skin tissue can have a diagnostic value.[3] Hence, there is a need to further determine how Mie and Rayleigh scattering varies in a larger cohort.

Previous characterizations of tissue scattering applied inverse photon propagation algorithms to sets of measured light intensities to estimate the optical properties of tissue (i.e., absorption and reduced scattering coefficients). Typically based on either the diffusion approximation or Monte Carlo simulations, these algorithms vary in complexity and may include: multiple layers with different μ_s',[7,8] absorbing chromophores with wavelength constraints,[9,10] and different degrees of Mie and Rayleigh scattering to properly account for the different scattering particle sizes found in tissue.[10] It has been shown that the accuracy of an inverse algorithm depends on how well the photon propagation model can mimic the detected light intensity.[11,12]

Different modalities for illumination and detection of light are commonly used when assessing optical properties. For *in vitro* studies, tissue samples may be analyzed using single- and double-integrating sphere setups.[13] *In vivo* setups may have a temporally[14] or spatially[15] modulated light source, or utilize multiple detection points in combination with a steady-state single-point light source.[16,17] In both *in vivo* and *in vitro* studies, the number of analyzed subjects or samples has been limited.[18] Furthermore, *in vitro* samples may have a higher μ_s', partly due to sample preparation.[4] Hence, to develop diagnostic and therapeutic optical modalities based on light transport modeling, there is a need for a more comprehensive dataset on μ_s'.

The aim of this study was to assess light scattering in the forearm skin of the subjects in the Linköping cohort of the Swedish CArdioPulmonary bioImage Study (SCAPIS). This is, to our knowledge, the first time tissue optical scattering

*Address all correspondence to: Hanna Jonasson, E-mail: hanna.jonasson@liu.se

has been estimated in such a large study. The magnitude and variation in a normal population can serve as input parameters when designing new inverse algorithms or when predicting the effect of therapeutic optical techniques.

Light scattering data were determined as the reduced scattering coefficient and the fraction of Mie and Rayleigh scattering. The scattering properties were assessed using an instrument integrating spatially resolved diffuse reflectance spectroscopy and laser Doppler flowmetry. Data analysis included an inverse Monte Carlo algorithm that in addition to scattering accounts for geometrical and absorbing properties of the tissue.

2 Methods

2.1 *Instrumentation*

The measurements were performed with a Periflux 6000 EPOS system (Enhanced Perfusion and Oxygen Saturation; Perimed AB, Järfälla, Stockholm, Sweden). The system consisted of a PF 6010 laser Doppler unit (including a laser light source at 785 nm and an optical passband filter 785 ± 40 nm), a PF 6060 spectroscopy unit, a broadband white light source (Avalight-HAL-S, Avantes BV, the Netherlands), and a fiber-optic probe. Only data from the spectroscopy unit were used to assess the scattering properties of skin in this study. The PF 6060 spectroscopy unit contained two spectrometers (AvaSpec-ULS2048L, Avantes BV, the Netherlands) and an optical notch filter suppressing wavelengths 790 ± 20 nm to minimize influences from the laser light source on DRS spectra. The fiber-optic probe included a white light-emitting fiber and two detecting fibers for DRS spectra placed at distances of 0.4 and 1.2 mm from the emitting fiber. The fibers connected to the white light source and the spectrometers had a core diameter of 200 μm, whereas the fibers connected to the PF 6010 laser Doppler module had a core diameter of 125 μm. All fibers had a numerical aperture of 0.37 and were made of fused silica.

2.2 *Skin Model*

The skin was modeled as a three-layered structure, including geometrical, absorption, and scattering properties. The top layer mimicked the epidermis with melanin as an absorber, whereas the two other layers represented shallow and deep dermis with hemoglobin at variable oxygen saturation levels as absorber.[19,20] Thus, the absorption coefficient differed between the layers, whereas the reduced scattering coefficient was assumed to be equal in all layers.

Scattering in tissue can be considered to originate from particles of a continuous range of sizes. The scattering caused by particles smaller than the wavelength of the light was modeled as Rayleigh scattering with a reduced scattering coefficient decaying exponentially with the power of −4. The scattering from particles that were of the same size as the wavelength or larger were modeled as Mie theory. Here a reduced scattering coefficient is exponentially decaying with the power of $-\beta$ ($0 < \beta < 4$). By combining these two scattering regimes, Jacques[4] suggested modeling the reduced scattering coefficient of skin as a function of the wavelength according to

$$\mu_s'(\lambda) = \alpha' \left[(1-\gamma) \left(\frac{\lambda}{\lambda_0}\right)^{-\beta} + \gamma \left(\frac{\lambda}{\lambda_0}\right)^{-4} \right], \quad (1)$$

where α' equals μ_s' at the reference wavelength ($\lambda_0 = 600$ nm), β is the Mie scattering decay, and γ ($0 \leq \gamma \leq 1$) describes the fraction of Rayleigh scattering. We have previously shown that this scattering model is capable of describing the reduced scattering in the 475- to 850-nm wavelength range well while reducing it to a simpler form containing only two parameters α' and β does not describe the scattering to a sufficient degree.[10]

Jacques[4] reported that melanin absorption can be described by an exponential equation as

$$\mu_{a,mel}(\lambda) = k \left(\frac{\lambda}{\lambda_0}\right)^{-\beta_{mel}}. \quad (2)$$

Multiplying that equation with the melanin fraction in epidermis (f_{mel}) gives the absorption coefficient of the epidermis layer in the skin model.

In total, the skin model contained 11 parameters affecting the diffuse reflectance spectra (and additional parameters for blood flow). One parameter was the epidermis layer thickness (t_{epi}), two parameters for melanin absorption (f_{mel} and β_{mel}), the three reduced scattering parameters α', β, and γ, two parameters for tissue fractions of red blood cells containing hemoglobin, two parameters for hemoglobin oxygen saturation, and one parameter for average vessel diameter. For further details about the skin model used, see Refs. 19 and 21.

2.3 *Inverse Monte Carlo*

An inverse Monte Carlo method is used in the EPOS system iteratively updating the 11 model parameters comparing measured and modeled DRS spectra at the two source-detector separations 0.4 and 1.2 mm, respectively. For a given set of model parameters, reduced scattering (same for all layers) and absorption (different for each layer) coefficients are calculated at each wavelength. The optical path-length distributions within each layer of this model are then determined by interpolating based on the epidermal thickness parameter and homogeneous reduced scattering coefficient over a range of precomputed layered Monte Carlo simulations. In those Monte Carlo simulations, the scattering anisotropy factor was set to 0.8. Finally, Beer–Lambert's law is applied for each path length in the interpolated path-length distributions to account for the absorption effect. The modeled intensities at each wavelength, i.e., the modeled DRS spectra, are then compared with the measured spectra. First, these modeled DRS spectra are normalized with the average intensity over both source–detector separations of the measured spectra, eliminating the need for absolute intensity calibration of the spectrometers. A nonlinear optimization using a trust region reflective algorithm is then employed to find the set of parameters that result in the best match between the measured and modeled DRS spectra. A detailed description of the inverse Monte Carlo method and how spectra are calculated from a given set of model parameters has been presented before Refs. 10 and 19.

2.4 *In Vivo Data*

Diffuse reflectance spectra in the wavelength range of 475 to 850 nm were measured from the volar forearm of 1765 men and women between 50 and 64 years, the majority with Caucasian skin types. All subjects participated at the Linköping site of the large multicenter study, SCAPIS. The rationale and methodology of SCAPIS have been described

previously.[22] SCAPIS has been approved as a multicenter trial by the ethics committee at Umeå University (Dnr 2010-228-31M with amendment, EPN Umeå) and adheres to the Declaration of Helsinki. The diffuse reflectance measurements and the analysis of data have been approved by the ethics committee in Linköping (Dnr 2018/156-31). Written informed consent was obtained from all subjects.

The subjects were asked to refrain from consuming large meals and coffee for 3 h, nicotine for 4 h, and alcohol for 12 h prior to the measurements. Medications were omitted on the morning of the study, except for anticoagulants, contraceptives, or medications for Parkinson's disease, diabetes, epilepsy, chronic pain, and spasticity. The subjects were acclimatized in a temperature-controlled room (23.7°C ± 0.5°C) and rested in a supine position for 15 min before the start of the measurements. A fiber optic probe was attached to the volar surface of the right arm using double-sided adhesive tape, avoiding visible veins, pigmented nevi, and hair. The protocol included five minutes baseline, 5 min arterial occlusion of the forearm using a blood pressure cuff rapidly inflated to 250 mmHg, and a 10-min reperfusion phase. Baseline, occlusion, and reperfusion values were calculated as the mean over each phase.

2.5 *Statistics*

Parameters are presented as mean ± standard deviation (SD). The 95% confidence intervals (CI) were calculated as mean ± 2 SD. Paired Student's t-test was used to test significant differences in the scattering parameters between the three phases (baseline, occlusion, and reperfusion). Independent sample Student's t-test was used when analyzing gender differences. Correlations were assessed using Pearson's correlation coefficient r. A p value <0.05 was considered as statistically significant. The significance of the parameter of interest is reported without adjustment for multiple testing. All analyses were performed using IBM SPSS version 25 (SPSS, Chicago, Illinois).

3 Results

Twenty-seven subjects were excluded due to data acquisition failure and four subjects decided to end the measurement before the end of the protocol. The age of the remaining 1734 study subjects was 57.7 ± 4.4 years (mean ± SD).

The average reduced scattering coefficient for baseline values in the wavelength range 475 to 850 nm, and their normal (± SD) variation are shown in Fig. 1. The mean μ_s' ranged from 3.16 (SD = 0.72) mm^{-1} at 475 nm to 1.13 (0.27) mm^{-1} at 850 nm (Table 1). The corresponding 95% confidence intervals for the reduced scattering coefficient are [1.71 to 4.60] mm^{-1} and [0.60 to 1.67] mm^{-1}, respectively (Table 1).

Mean baseline, occlusion, and reperfusion values for the parameters describing the reduced scattering coefficient [Eq. (1)] are shown in Table 2. There was a significant difference in the parameters α' and γ between the occlusion and reperfusion phases compared with baseline ($p < 0.001$).

The baseline histograms for α', β, and γ are shown in Figs. 2(a)–2(c). It can be observed that the distribution for β is right skewed, whereas that for γ is left skewed.

All the following analyses were performed only for baseline values. Age was correlated to α' ($p < 0.001$, $r = -0.12$). The total amount of melanin (melanin concentration times epidermis thickness) was on average 0.48% ± 0.36% mm and correlated to α ($p < 0.001$, $r = -0.32$), β ($p < 0.001$, $r = 0.57$), and γ ($p = 0.004$, $r = -0.069$).

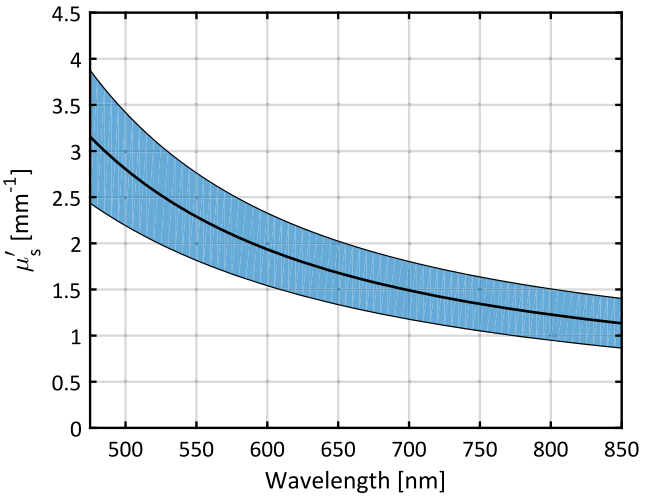

Fig. 1 Average reduced scattering coefficient during baseline (middle line) with the shaded area marking ±1 SD.

Table 1 The reduced scattering coefficient in baseline as mean [mm^{-1}], SD, and 95% confidence interval.

Wavelength [nm]	Mean [mm^{-1}]	1 SD	95% CI
475	3.16	0.72	1.71 to 4.60
500	2.80	0.61	1.58 to 4.03
525	2.52	0.53	1.45 to 3.59
550	2.29	0.47	1.34 to 3.24
575	2.10	0.43	1.24 to 2.95
600	1.93	0.39	1.15 to 2.72
625	1.80	0.37	1.07 to 2.53
650	1.68	0.34	0.99 to 2.37
675	1.58	0.33	0.92 to 2.23
700	1.49	0.31	0.86 to 2.12
725	1.41	0.30	0.81 to 2.02
750	1.34	0.29	0.76 to 1.93
775	1.28	0.28	0.71 to 1.85
800	1.23	0.28	0.67 to 1.78
825	1.18	0.27	0.63 to 1.72
850	1.13	0.27	0.60 to 1.67

There were significant differences in all scattering parameters between men and women ($p < 0.001$), Table 3. No significant difference in the amount of melanin among men and women was observed.

4 Discussion

In this study, we present *in vivo* scattering properties of human skin in a large Swedish cohort. The results, describing the

Table 2 Parameters describing the reduced scattering coefficient during the three phases.

	Baseline	Occlusion	Reperfusion	*p*
α' [mm^{-1}]	1.93 ± 0.39	1.95 ± 0.40*	2.02 ± 0.43*	<0.001
β [-]	0.940 ± 0.487	0.939 ± 0.494	0.947 ± 0.466	n.s.
γ [-]	0.277 ± 0.144	0.284 ± 0.140*	0.260 ± 0.139*	<0.001

Note: Data are given as mean ± SD. n.s. not significant.
*Significant difference compared to baseline.

magnitude and variation in the reduced scattering coefficient in a normal population, can be used as an input when developing inverse algorithms, when predicting the effect of therapeutic optical techniques, or when evaluating traumatzed skin including burn wound assessment.[6] In addition, we have also assessed the influences of gender and age on the parameters describing the reduced scattering coefficient in tissue and the correlation between the reduced scattering coefficient and the amount of melanin.

The EPOS system, along with its skin model and inverse Monte Carlo method, has been designed to measure oxygen saturation, RBC tissue fraction, and speed-resolved perfusion. Previous studies using the EPOS system have only reported these specific output parameters.[19,21,23,24] This article, however, is focused on extracting and reporting scattering properties using this system. A previous validation has shown that the accuracy of the EPOS method in estimating the reduced scattering coefficient was within 15% using two-layered silicon phantoms including TiO_2 as a scattering agent.[25] We have reasons to believe that the error is smaller than this as the optical phantoms in the evaluation contained a hemoglobin mimicking absorber with much less prominent absorption peaks than that of real hemoglobin. This makes the data fitting of the inverse Monte Carlo method more difficult. Furthermore, it should be noted that the values of reduced scattering in the validation study (range 1.25 to 3 mm^{-1}) resembled those observed in the present study.

Previously reported values on μ_s' originate from both *in vitro* and *in vivo* studies. Bashkatov et al.[13] examined 23 *in vitro* postmortem skin samples in a double-integrating sphere system. They observed a μ_s' ranging from 4.1 to 1.9 mm^{-1} in the 475- to 850-nm wavelength range. Salomatina et al.[5] analyzed eight dermis samples *in vitro*. Their μ_s' ranged from 4.8 to 2.1 mm^{-1}. Jacques[4] compiled data from eight studies (both *in vitro* and *in vivo*) including Bashkatov[13] and found μ_s' in the range 5.4 to 2.2 mm^{-1}. Bosschaart et al.[17] examined 60 neonates' dorsal hand skin using *in vivo* spatially resolved diffuse reflectance and found μ_s' ranging approximately from 2.7 to 1.3 mm^{-1} in 450 to 600 nm. Our range of 3.16 to 1.13 mm^{-1} for the reduced scattering coefficient in the 475- to 850-nm wavelength range is in line with these studies. The difference between studies is larger regarding the individual parameters (α', β, and γ) describing the reduced scattering coefficient.[4]

There was a small, but significant, deviation from baseline values in the parameter α' and γ during the arterial occlusion and reperfusion phases. This could be an effect of the scattering model, where all layers are assumed to have equal scattering properties. If scattering varies as a function of depth in skin, a change in the sampling volume might change the scattering

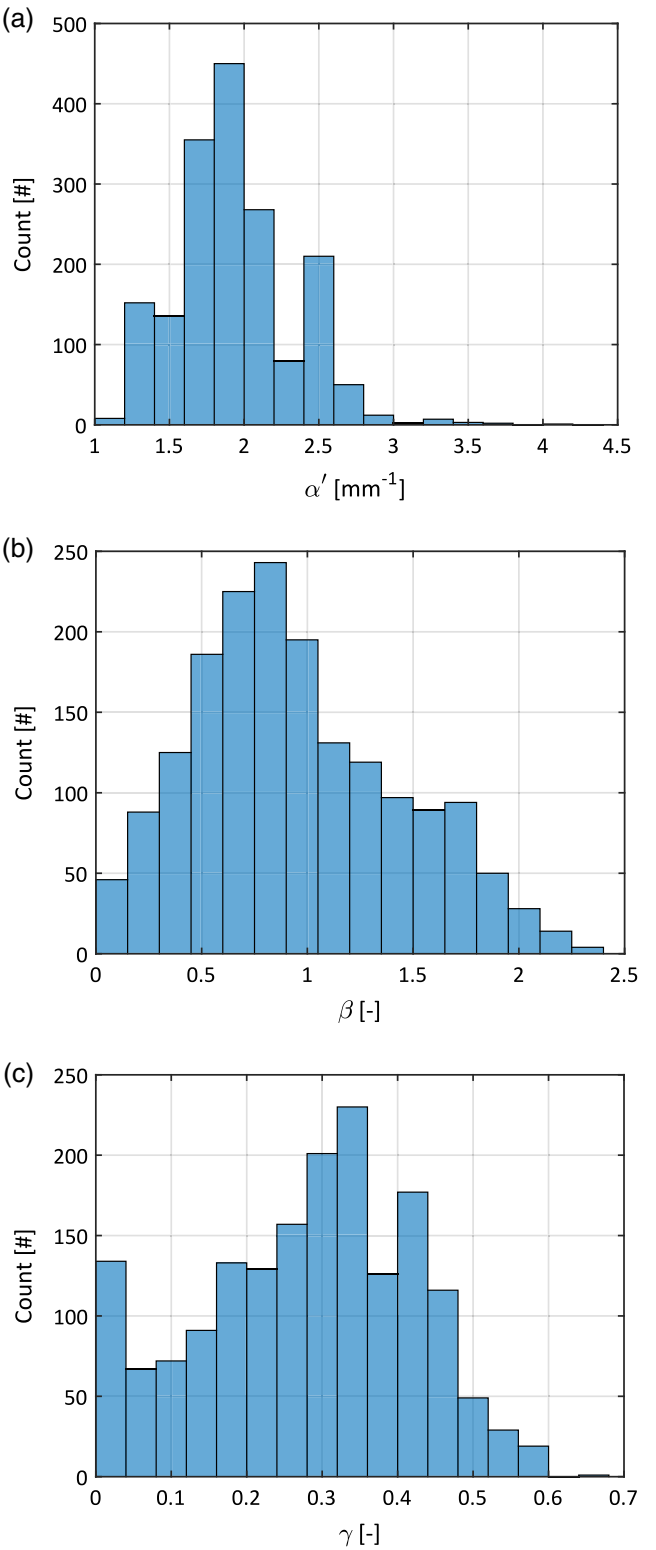

Fig. 2 Histograms for the parameters (a) α', (b) β, and (c) γ. Time-averaged parameter value during 5-min baseline.

parameters during the provocation as the model cannot account for different scattering properties in different layers. This could result from a different amount of blood due to a redistribution of blood between the layers during the occlusion and reperfusion phases. More work is needed to determine whether the change is a model effect or relates to an actual change in scattering

Table 3 Differences in scattering parameters between men and women.

	Men ($n = 892$)	Women ($n = 842$)	P
α' [mm^{-1}]	1.98 ± 0.40	1.89 ± 0.38	<0.001
β [-]	1.01 ± 0.48	0.86 ± 0.48	<0.001
γ [-]	0.25 ± 0.14	0.30 ± 0.14	<0.001

Note: Data are given as mean ± SD.

properties during a provocation. Even though the deviation from baseline is small, it is present for the majority of the individuals included in this study.

Melanin is recognized as an important absorbing component in skin, but the impact of melanin on tissue scattering has not been fully clarified. Sardar et al.[26] investigated the optical properties of melanin *in vitro* and found that the scattering coefficient of melanin was much higher than the absorption coefficient for wavelengths between 476 and 633 nm. On the other hand, Zonios and Dimou[27] found no difference in scattering properties when comparing normal skin and pigmented nevi, and concluded that melanin had negligible impact on skin scattering. The number of subjects in that study was; however, small ($n = 3$) and the linear model for scattering did not account for Rayleigh scattering. We found a correlation between total amount of melanin, estimated from the model, and the scattering properties of skin, especially for the α' and β parameters, where α' characterizes scattering density and β is the size of the scattering particles. Our findings showed that the reduced scattering coefficient and the size of the scattering particles decreased with an increased amount of melanin, which is in line with previous findings by Tseng et al.[28] They related the reduction in μ_s' to a smaller sampling volume as more light gets absorbed as the amount of melanin increases, where fewer photons would have passed a smaller volume of scattering particles like collagen and elastin in the dermis. An increase in the β indicates a shift toward smaller structures scattering within the sampled volume. Riesz et al.[29] found that the scattering coefficient of melanin *in vitro* applies to Rayleigh theory for wavelengths between 210 and 325 nm. *In vivo* melanin is located in melanosomes, with various sizes and distributions; however, the relationship between *in vitro* and *in vivo* scattering of melanin is not clear.

In this study, we found both a correlation between the reduced scattering coefficient and age, and significant differences in all scattering parameters between men and women, resulting in a lowered reduced scattering coefficient for women. Saidi et al.[30] found a positive correlation between μ_s' and age in neonates, where the reduced scattering coefficient increased as the density of collagen fibers increased during maturation. Bosschaart et al.[17] found no correlation between age in neonates and μ_s'. They related the lack of correlation to an age range outside the one used in their study as μ_s' is expected to increase at some point during maturation and be higher in adults.[4] The negative correlation between μ_s' and age could originate from the decrease in collagen concentration in skin during aging.[31] Women also have a lower collagen concentration compared with men,[31,32] which could cause the differences between men and women in all scattering parameters. Few previous studies have reported gender differences in the reduced scattering coefficient in human skin, probably due to small numbers of subjects. Calabro et al.[33] showed a lower reduced scattering coefficient in the skin of female mice, which was found to be related to a thinner dermal layer for females caused by less collagen.

5 Conclusions

In this study, *in vivo* values for tissue scattering are presented from a cohort including 1734 subjects. This is the first time these type of data have been presented for such a large number of included subjects. Within the cohort, we found a negative correlation between the reduced scattering coefficient and age, and a significant difference between men and women in the reduced scattering coefficient as well as in the fraction of small scattering particles. Our presented mean values for reduced scattering are well in line with many previously reported values. In addition, we also report on the distribution of the α', β, and γ parameters, describing the reduced scattering coefficient, which may serve as reference values for future studies.

Disclosures

Dr. Fredriksson is part-time employed by Perimed AB, which is developing products related to research described in this publication.

Acknowledgments

This study was supported by Sweden's innovation agency VINNOVA via the program MedTech4Health (d.no. 2016-02211). The baseline examination of SCAPIS was supported in full by the Swedish Heart and Lung Foundation; the study is also funded by the Knut and Alice Wallenberg Foundation, the Swedish Research Council and VINNOVA.

References

1. S. T. Flock et al., "Monte Carlo modeling of light propagation in highly scattering tissues. I. Model predictions and comparison with diffusion theory," *IEEE Trans. Biomed. Eng.* **36**(12), 1162–1168 (1989).
2. T. Lister, P. A. Wright, and P. H. Chappell, "Optical properties of human skin," *J. Biomed. Opt.* **17**(9), 090901 (2012).
3. J. R. Mourant et al., "Mechanisms of light scattering from biological cells relevant to noninvasive optical-tissue diagnostics," *Appl. Opt.* **37**(16), 3586–3593 (1998).
4. S. L. Jacques, "Optical properties of biological tissues: a review," *Phys. Med. Biol.* **58**(11), R37–R61 (2013).
5. E. V. Salomatina et al., "Optical properties of normal and cancerous human skin in the visible and near-infrared spectral range," *J. Biomed. Opt.* **11**(6), 064026 (2006).
6. A. Ponticorvo et al., "Quantitative long-term measurements of burns in a rat model using spatial frequency domain imaging (SFDI) and laser speckle imaging (LSI)," *Lasers Surg. Med.* **49**(3), 293–304 (2017).
7. Q. Liu and N. Ramanujam, "Sequential estimation of optical properties of a two-layered epithelial tissue model from depth-resolved ultraviolet-visible diffuse reflectance spectra," *Appl. Opt.* **45**(19), 4776–4790 (2006).
8. Q. Wang, K. Shastri, and T. J. Pfefer, "Experimental and theoretical evaluation of a fiber-optic approach for optical property measurement in layered epithelial tissue," *Appl. Opt.* **49**(28), 5309–5320 (2010).
9. G. M. Palmer and N. Ramanujam, "Monte Carlo-based inverse model for calculating tissue optical properties. Part I: theory and validation on synthetic phantoms," *Appl. Opt.* **45**(5), 1062–1071 (2006).
10. I. Fredriksson, M. Larsson, and T. Strömberg, "Inverse Monte Carlo method in a multilayered tissue model for diffuse reflectance spectroscopy," *J. Biomed. Opt.* **17**(4), 047004 (2012).

11. H. Karlsson et al., "Can a one-layer optical skin model including melanin and inhomogeneously distributed blood explain spatially resolved diffuse reflectance spectra?" *Proc. SPIE* **7896**, 78962Y (2011).
12. T. Lindbergh et al., "Improved model for myocardial diffuse reflectance spectra by including mitochondrial cytochrome aa3, methemoglobin, and inhomogenously distributed RBC," *J. Biophotonics* **4**(4), 268–276 (2011).
13. A. N. Bashkatov et al., "Optical properties of human skin, subcutaneous and mucous tissues in the wavelength range from 400 to 2000 nm," *J. Phys. D Appl. Phys.* **38**(15), 2543–2555 (2005).
14. B. J. Tromberg et al., "Non-invasive measurements of breast tissue optical properties using frequency-domain photon migration," *Philos. Trans. R. Soc. London Ser. B* **352**(1354), 661–668 (1997).
15. D. J. Cuccia et al., "Quantitation and mapping of tissue optical properties using modulated imaging," *J. Biomed. Opt.* **14**(2), 024012 (2009).
16. M. Larsson, H. Nilsson, and T. Strömberg, "In vivo determination of local skin optical properties and photon path length by use of spatially resolved diffuse reflectance with applications in laser Doppler flowmetry," *Appl. Opt.* **42**(1), 124–134 (2003).
17. N. Bosschaart et al., "Optical properties of neonatal skin measured in vivo as a function of age and skin pigmentation," *J. Biomed. Opt.* **16**(9), 097003 (2011).
18. A. N. Bashkatov, E. A. Genina, and V. V. Tuchin, "Optical properties of skin, subcutaneous, and muscle tissues: a review," *J. Innovative Opt. Health Sci.* **4**(1), 9–38 (2011).
19. I. Fredriksson et al., "Inverse Monte Carlo in a multilayered tissue model: merging diffuse reflectance spectroscopy and laser Doppler flowmetry," *J. Biomed. Opt.* **18**(12), 127004 (2013).
20. T. Strömberg, F. Sjöberg, and S. Bergstrand, "Temporal and spatiotemporal variability in comprehensive forearm skin microcirculation assessment during occlusion protocols," *Microvasc. Res.* **113**, 50–55 (2017).
21. T. Strömberg et al., "Microcirculation assessment using an individualized model for diffuse reflectance spectroscopy and conventional laser Doppler flowmetry," *J. Biomed. Opt.* **19**(5), 057002 (2014).
22. G. Bergström et al., "The Swedish CArdioPulmonary BioImage Study: objectives and design," *J. Intern. Med.* **278**(6), 645–659 (2015).
23. H. Jonasson et al., "Oxygen saturation, red blood cell tissue fraction and speed resolved perfusion—a new optical method for microcirculatory assessment," *Microvasc. Res.* **102**, 70–77 (2015).
24. H. Jonasson et al., "Skin microvascular endothelial dysfunction is associated with type 2 diabetes independently of microalbuminuria and arterial stiffness," *Diabetes Vasc. Dis. Res.* **14**(4), 363–371 (2017).
25. I. Fredriksson et al., "Evaluation of a pointwise microcirculation assessment method using liquid and multilayered tissue simulating phantoms," *J. Biomed. Opt.* **22**(11), 115004 (2017).
26. D. K. Sardar, M. L. Mayo, and R. D. Glickman, "Optical characterization of melanin," *J. Biomed. Opt.* **6**, 404–411 (2001).
27. G. Zonios and A. Dimou, "Light scattering spectroscopy of human skin in vivo," *Opt. Express* **17**(3), 1256–1267 (2009).
28. S.-H. Tseng, A. Grant, and A. J. Durkin, "In vivo determination of skin near-infrared optical properties using diffuse optical spectroscopy," *J. Biomed. Opt.* **13**(1), 014016 (2008).
29. J. Riesz, J. Gilmore, and P. Meredith, "Quantitative scattering of melanin solutions," *Biophys. J.* **90**(11), 4137–4144 (2006).
30. I. S. Saidi, S. L. Jacques, and F. K. Tittel, "Mie and Rayleigh modeling of visible-light scattering in neonatal skin," *Appl. Opt.* **34**(31), 7410–7418 (1995).
31. S. Shuster, M. M. Black, and E. McVitie, "The influence of age and sex on skin thickness, skin collagen and density," *Br. J. Dermatol.* **93**(6), 639–643 (1975).
32. H. Dao, Jr. and R. A. Kazin, "Gender differences in skin: a review of the literature," *Gender Med.* **4**(4), 308–328 (2007).
33. K. Calabro et al., "Gender variations in the optical properties of skin in murine animal models," *J. Biomed. Opt.* **16**(1), 011008 (2011).

Biographies for the authors are not available.